

MSLED: The Micro Subglacial Lake Exploration Device

Alberto E Behar*^{1,2}, Daming D Chen**², Colin Ho², Emily McBryan², Christian Walter¹, Joseph Horen², Scott Foster², Tyler Foster², Andrew Warren², Sai H Vemprala² and James M Crowell²

¹NASA Jet Propulsion Laboratory, 4800 Oak Grove Drive, Pasadena, CA, 91109-8099, USA

²School of Earth and Space Exploration, Arizona State University, PO Box 871404, Tempe, AZ 85287-6004, USA

Received 31 December 2014; Accepted 8 May 2015

Abstract

Satellite altimetry and ice-penetrating radar have shown the existence of active subglacial lakes in Antarctica which may have a significant impact on the Southern Ocean and the dynamics of the overlying ice sheet. Understanding how subglacial floods affect ice dynamics is imperative to predicting the effect of ice sheets on rising sea levels, but it is not clearly understood. Furthermore, these encapsulated lakes contain uncharacterised biological ecosystems and serve as analogue environments for future extraterrestrial exploration. To investigate these subglacial environments, the authors developed the Micro Subglacial Lake Exploration Device (MSLED), a unique highly-miniaturised remotely operated vehicle. Equipped with a high-resolution imaging system, as well as conductivity, temperature and depth sensors for *in situ* measurements, the MSLED is capable of determining geological, hydrological and biological characteristics of subglacial lakes. It was successfully deployed in Antarctica during the 2011–2012 and 2012–2013 Antarctic summer seasons in collaboration with the Whillans Ice Stream Subglacial Access Research Drilling (WISSARD) expedition to Subglacial Lake Whillans (SLW), contributing to the discovery of microbial ecosystems within these environments. The present paper outlines the scientific background behind the mission, the design and implementation of the MSLED, as well as the results of tests and initial deployments in Antarctica.

Keywords: extreme environments, marine robotics, planetary robotics, underwater robotics, subglacial lakes

1. Introduction

1.1. Antarctic subglacial lakes

Melting of the Antarctic ice sheet, which contains 61% of Earth's fresh water, has a direct effect on sea

level and freshwater input to the Southern Ocean. A complete melting of the West Antarctic Ice Sheet would contribute approximately 3.3m to global sea level rise (Bamber et al., 2009). As a result, despite existing knowledge about the cryosphere, further investigations are necessary in order to better understand the complex processes of this environment.

Detection of active subglacial lakes in West Antarctica by satellite radar interferometry (Gray et al., 2005), laser altimetry (Fricker et al., 2007) and radio-echo sounding (Wingham et al., 2006) have led to an inventory of 124 active lakes throughout Antarctica (Smith et al., 2009; Wright and Siegert, 2012). It is known that subglacial water and wet sediments, acting as lubricants, can impact ice stream flow in Antarctica (Kamb, 1987). Predicting the future of ice sheets and their effect on rising sea levels will require a better understanding of these subglacial systems (Alley, 2001; Fricker et al., 2007; Siegert et al., 2005). In particular, processes at the basal ice sheet boundary, and at the ice-ocean interface that govern the rate of ice loss to the ocean, are still insufficiently understood to be incorporated into ice sheet models (Vaughan and Arthern, 2007).

Subglacial sediments contain a record of microbial activity under the ice sheet. Although estimates of bacterial abundance within the Antarctic ice sheet indicate the presence of a previously unrecognised carbon pool (Priscu and Christner, 2004), past discoveries of microbial life in subglacial sediments (Christner et al., 2006; Lanoil et al., 2009) have been controversial. Frozen water samples recovered from Subglacial Lake Vostok (SLV) were contaminated by a hydrocarbon drilling fluid (Karl et al., 1999) necessitating additional data collection using

* Deceased 9 January 2015

** Contact author. Email address: ddchen@asu.edu

microbiologically clean techniques (Priscu et al., 2013). Although data from Subglacial Lake Whillans (SLW) indicate the presence of microbial life (Christner et al., 2014), further examination of these benthic communities is necessary to determine potential sources of nutrients and energy, as well as the microbial processes beneath large ice shelves (Domack et al., 2005).

In addition, these subglacial environments also serve as potential analogues for the exploration of extraterrestrial bodies such as Europa, one of Jupiter's moons, which is believed to contain a subsurface ocean beneath its icy crust (Lorenz et al., 2011).

1.2. Whillans Ice Stream Subglacial Access Research Drilling

The Whillans Ice Stream Subglacial Access Research Drilling (WISSARD) initiative, funded by the US National Science Foundation, carried out a hydrological study of the Whillans Ice Stream in West Antarctica over a six-year period from 2009 through 2015. This location was selected because of its proximity to three distinct environments interconnected by the exchange of water and sediments: the sub-ice shelf cavity, the grounding-zone wedge and Subglacial Lake Whillans (Fricker et al., 2011). As such, this initiative was composed of three integrated projects: one that focused on exploring the GeomicroBiology of the Antarctic Subglacial Environment (GBASE); one that provided Robotic Access to Grounding-zones for Exploration and Science (RAGES); and one based on Lake and Ice Stream Subglacial Access Research Drilling (LISSARD).

Of particular interest was Subglacial Lake Whillans (SLW), an active subglacial lake located nominally 800m beneath the surface of the ice (Christianson et al., 2012), which experiences fill-and-drain cycles

on the order of years to decades. Fed by glacial ice melt from the Mercer and Whillans Ice Streams, SLW fluctuates in water depth between approximately 8–15m (Fricker et al., 2007), discharging to a subglacial estuary connected to the ice-water cavity beneath the Ross Ice Shelf (Horgan et al., 2013).

As part of the LISSARD subproject a hot water drilling system created an opening into the ice sheet near the edge of SLW that was reamed out to a diameter of ~60cm (Rack et al., 2014; Blythe et al., 2014; Burnett et al., 2014). The actual mission diameter was set at 30cm in order to account for lateral borehole refreezing (Priscu et al., 2013; Christner et al., 2014). During deployment all equipment that entered the pristine environment underwent chemical decontamination with aqueous hydrogen peroxide and ultraviolet radiation (Priscu et al., 2013) before being lowered into the subglacial lake through this borehole.

At the time of drilling in late January 2013 the lake was near minimum depth having discharged 4m in 2008 to 2009 (Tulaczyk et al., 2014). Results from that study indicated that the water column of SLW contains metabolically active microorganisms and solute from both lithogenic weathering and sea water, confirming that Antarctic subglacial lakes contain globally-relevant pools of carbon and microbes (Christner et al., 2014).

1.3. Remotely operated vehicles

To collect information about the subglacial environment a large variety of remotely operated vehicles (ROVs) or autonomous underwater vehicles (AUVs) are available commercially, academically, or are currently under development (Antonelli et al., 2008). Table 1 lists a selection of relevant vehicles for the mission presented subsequently in section 2 of the

Table 1: Selection of similar underwater vehicles

Manufacturer	Vehicle	Dimensions (m)	Depth (m)	CTD	Selected imaging
Bluefin Robotics Co.	Bluefin-9	0.24 × 1.65	200	Yes	Optical, Sonar, DVL
Bluefin Robotics Co.	Bluefin-12S	0.32 × 3.77	200	Yes	Sonar, DVL
Deep Ocean Exploration and Research	Sub-Ice Rover	8.5 × 0.56	1,500	Yes	Optical, Sonar, ADCP
Georgia Tech	Icefin	N/A	1,500	N/A	Optical, Sonar, ADCP
Kongsberg Maritime	Remus 100	0.19 × 1.6	100	Yes	Optical, Sonar, ADCP
Kongsberg Maritime	Remus 600	0.32 × 3.25	600	Yes	Optical, Sonar, ADCP
Kongsberg Maritime	Remus 6000	0.66 × 3.99	6,000	Yes	Optical, Sonar, ADCP
Kongsberg Maritime	Seaglider	0.3 × 1.8	1,000	Yes	ADCP
iRobot	15A Ranger	0.122 × N/A	N/A	N/A	Optical, Sonar
Moss Landing Marine Lab.	SCINI	0.15 × 1.4	300	Yes	Optical, Sonar
STONE Aerospace	ENDURANCE	2.13 × 1.52	1,000	Yes	Optical, Sonar, ADCP
Subglacial Lake Ellsworth Consortium	ESL Probe	0.2 × 3.5	4,000	Yes	Optical, Sonar, DVL
Teledyne Gavia	Gavia Scientific	0.2 × 1.8	1,000	Yes	Optical, Sonar, ADCP
VideoRay, LLC	Pro 4	0.38 × 0.29 × 0.22	300	TD	Optical, Sonar
Woods Hole Oceanographic Institute	Nereus	4.25 × 2.3 × 2.4	11,000	Yes	Optical, Sonar, ADCP
Woods Hole Oceanographic Institute	SeaBED	2.0 × 1.5 × 1.5	2,000	Yes	Optical, Sonar, ADCP
University of Nebraska Lincoln	Deep-SCINI	0.23 × 2.0	1,500	Yes	Optical

present paper including their relevant features such as dimensions, optical/sonar imaging capabilities and the presence of conductivity, temperature and depth sensors. Among these a number have been developed specifically for exploring subglacial lakes in Antarctica such as the Environmentally Non-Disturbing Under-ice Robotic Antarctic Explorer (ENDURANCE), an AUV deployed to Lake Bonney in 2007 and 2008 (Richmond et al., 2011), the Submersible Capable of under Ice Navigation and Imaging (SCINI), an ROV deployed to the Ross Ice Shelf from 2007 to 2009 (Cazenave et al., 2011), and the Ellsworth Subglacial Lake (ESL) Probe which was a non-maneuverable probe designed for measuring Subglacial Lake Ellsworth in 2012 (Mowlem et al., 2011). More recently, a number of ROVs with similar physical dimensions and depth ratings to MSLED have been developed for through-borehole deployment into deepwater environments. These include: Icefin at Georgia Tech, Deep-SCINI at the University of Nebraska Lincoln/Moss Landing Marine Laboratory and the Sub-Ice Rover at Deep Ocean Exploration and Research/Northern Illinois University; all have also undergone deployment in conjunction with the WISSARD expedition. The present paper outlines the design and implementation of the MSLED, including an examination of the differences between MSLED and the aforementioned vehicles, as well as the results of tests and initial deployments in Antarctica.

2. Mission

2.1. Objectives

As part of the LISSARD subproject, the Micro Subglacial Lake Exploration Device (MSLED) was developed to improve the understanding of Antarctic subglacial aquatic systems and their influence on ice stream dynamics. Since knowledge on those environments is limited, the mission objectives were exploratory and comprised: investigations of the ice-water interface, examining the distribution of entrained debris in basal ice, and observing the geometry of the ice-water interface; measurements of the distribution of physical (e.g. temperature, pressure) and chemical (e.g. salinity) parameters within the lake; visual inspections of the water column for suspended particles and possible aquatic organisms; searches for visual evidence of water stratification and horizontal and/or vertical motion; investigations of the lake floor for evidence of erosion and sedimentary processes (e.g. glacial flutings, subaqueous sediment failures, debris flows, deltas, drainage channels); and recordings of signs of possible bioturbation and/or benthic organisms.

2.2. Deployment setup

The deployment setup comprised the MSLED, a mothership that supported the MSLED during its descent and ascent, and a ground station at the surface, in addition to the drilling equipment and other scientific payloads deployed as part of the WISSARD expedition. This is shown in Fig 1.

After completion of the borehole the MSLED mothership was independently deployed for visual inspection of the borehole and subglacial cavity, followed by scientific instrumentation prioritised in descending diameter order such as the CTD profiler, water sampler, UWITEC multi-corer, geothermal probe, borehole sensor string and MSLED (Tulaczyk et al., 2014). During deployment all equipment entering the pristine environment underwent chemical decontamination with aqueous hydrogen peroxide and ultraviolet radiation (Priscu et al., 2013) before being lowered into the subglacial lake through this borehole. The MSLED was permanently connected to the ground station via the mothership through a fibre-optic communication system allowing it to transmit sensor data to the surface and receive remote commands from the ground station.

The mothership was anchored to the surface by a steel cable and a multi-fibre Kevlar-reinforced tether. In addition to serving as a communications intermediary the mothership also functioned as a docking station for the MSLED during ascent and descent. The mothership was furthermore equipped with a separate sensing package capable of visually inspecting the borehole and determining its depth.

Once the mothership descended into the subglacial lake the MSLED detached upon surface command allowing for independent exploration away from the mothership while maintaining two-way communications with the surface control station through the mothership. After completing the deployment mission the MSLED reattached to the mothership docking mechanism and was winched back to the surface.

3. System requirements

Based on the mission objectives and constraints of the WISSARD expedition, two respective sets of requirements were derived for the MSLED and its mothership.

3.1. MSLED

The MSLED was constructed based on the following list of design criteria. It had to be capable of:

- providing high-resolution video of at least $1,280 \times 1,024$ pixel resolution to the surface;

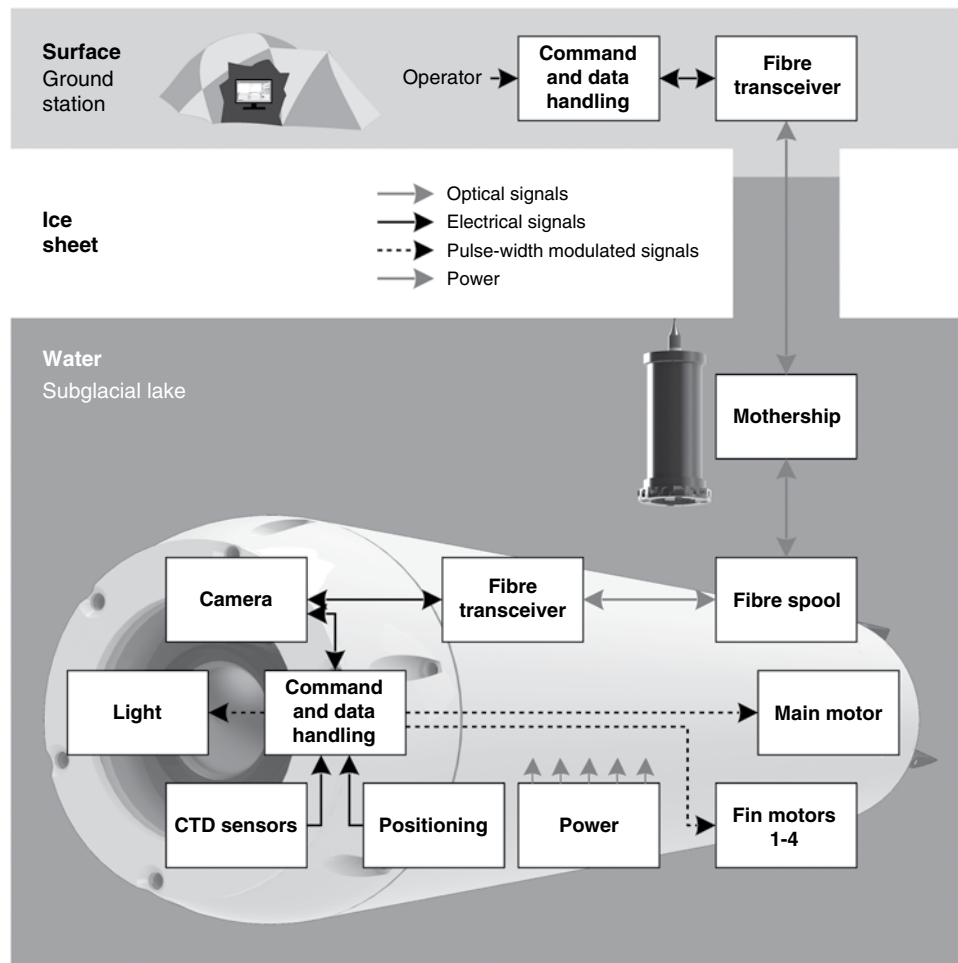


Fig 1: Overview of the deployment concept

- performing *in situ* measurements of temperature, salinity and pressure;
 - navigating a distance of up to 1km from lake access;
 - operating at a depth of down to 1.2km;
 - having a maximum diameter of 14cm and a maximum length of 70cm;
 - operating in low temperatures to a minimum of -4°C ;
 - continuously running on battery power for a minimum of two hours;
 - communicating bidirectionally with the surface at sufficient bandwidth to simultaneously transmit instrument data and high-definition video from the vehicle as well as receive operator commands from the surface in real time;
 - returning to the mothership prior to retrieval through the borehole; and
 - withstanding decontamination for clean deployment.
- 3.2. Mothership
- The mothership was designed to be capable of:
- supporting the deployment and retrieval of the MSLED vehicle;
 - operating independently from the MSLED;
 - visually inspecting the ice borehole and measuring its depth;
 - including bottom and side-facing high-resolution video recording systems of $1,920 \times 1,080$ pixels;
 - incorporating depth and inclination sensing;
 - operating at a depth of up to 900m;
 - being a maximum size of 20cm in diameter and 70cm in length;
 - operating in temperatures from -10°C to $+50^{\circ}\text{C}$;
 - functioning on battery power for a minimum of two hours with all subsystems operational;
 - communicating in full-duplex with the surface at sufficient bandwidth to simultaneously receive operator commands and transmit real-time instrument data, as well as high-definition video;
 - supporting external charging and access to camera and log data without disassembly;
 - recording all sensor measurements in a log file; and
 - withstanding decontamination for clean deployment.

3.3. Discussion

Owing to the technical requirements of this mission, the MSLED was custom-developed for exploring the extreme environment of SLW (Behar et al., 2010). Other vehicles that were, or could have been, considered for this mission are listed in Table 1. Many previous through-ice exploration vehicles were designed only for surface deployment and are, therefore, not suitable for subglacial deployment because of the depth requirements. For example, the Submersible Capable of under Ice Navigation and Imaging (SCINI) was rated for depths of up to 300m (Cazenave et al., 2011), while MSLED is rated for up to 1,200m. Even in comparison with similar deep exploration vehicles, the MSLED is still smaller; for example, the deep-ice successor of SCINI currently under development, Deep-SCINI, is rated for 1,500m depth but has a diameter of 23cm and a length of 2m. Likewise, although both the Nereus and Remus 6000 are respectively rated for 11,000m and 6,000m (Bowen et al., 2008), they were not designed for through-borehole deployment and exceeded the current mission dimensions. In addition, for the British Lake Ellsworth Programme, an Ellsworth Subglacial Lake (ESL) Probe was developed specifically as a self-contained probe rated to 4,000m (Mowlem et al., 2011), but it was incapable of movement and, thus, was not suitable for this mission. Furthermore, while several autonomous vehicles have been designed for underwater exploration, such as the Sub-Ice Rover and ENDURANCE, which contain additional instrumentation and are capable of image processing and simultaneous localisation and mapping (SLAM),

they exceeded the dimensions of the current mission significantly.

4. System design

The exterior and interior designs of both the assembled MSLED and the mothership are illustrated in Figs 2 and 3.

4.1. Structure and buoyancy

The mechanical structure of the MSLED consisted of several isolated compartments: a front pressure compartment, a middle fibre bay and a rear tail-cone (Fig 2). Nitrile rubber O-rings were used to provide pressure isolation of each compartment, with all inter-compartmental signaling connected through pressure-resistant feed-throughs.

The front pressure compartment housed all of the sensitive electronic and optical components within MSLED at surface pressure. This assembly consisted of a hard anodised (type III) thin wall cylindrical hull with a thickness of 3mm and a diameter of 80mm constructed from 7075-T6 aluminum alloy. This was corrosion resistant and less affected by pressure deformation than comparable alloys. A front nosecone held a 6.22mm-thick synthetic sapphire window that acted as the primary viewport for the video camera. At the rear, a pressure bulkhead sealed this main compartment from the flooded fibre bay and accommodated the electrical and fibre-optic pressure feed-throughs. The fibre feed-through was constructed out of a countersunk stainless steel bolt filled with 3M Scotchcast 4, while the electrical feed-throughs utilised Teledyne

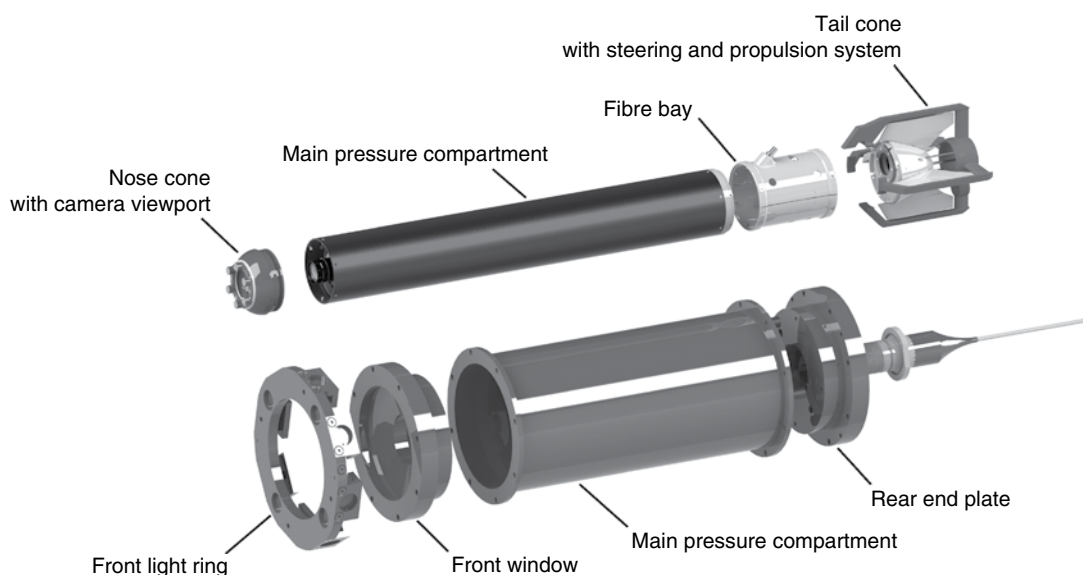


Fig 2: Exterior render of the MSLED (top) and mothership (bottom) showing the respective pressure compartments

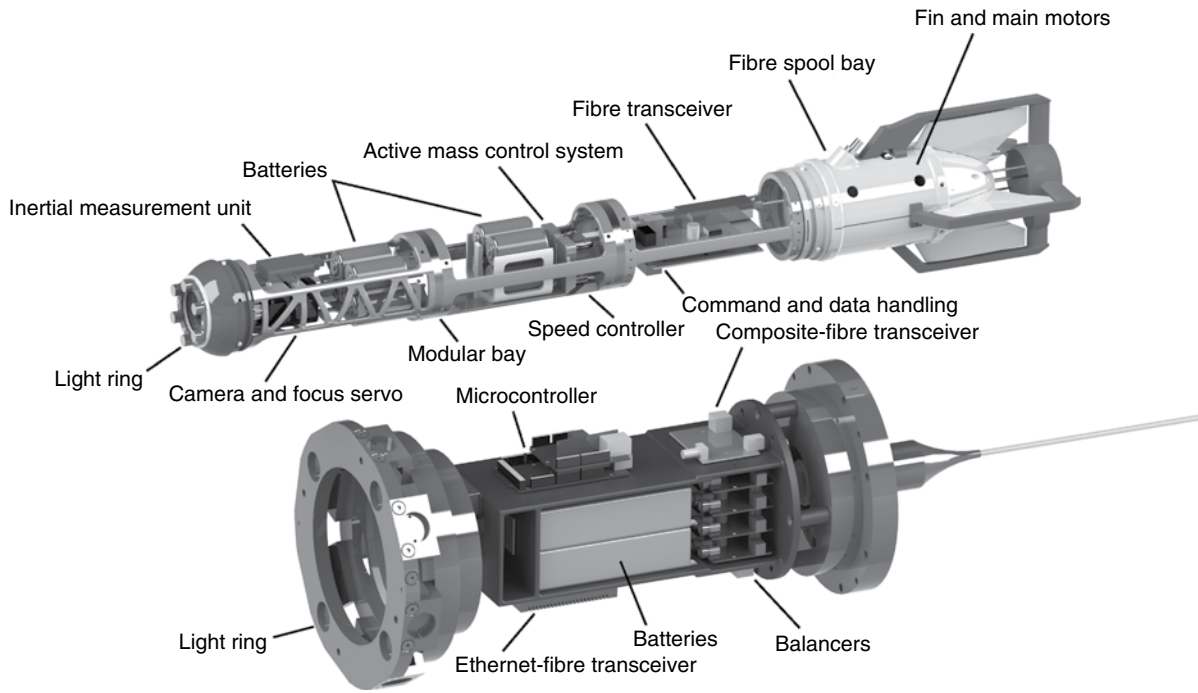


Fig 3: Interior render of the MSLED (top) and mothership (bottom) showing the 3D-printed internal structure

Impulse IE55-1206-CCP connectors, with each connector rated to 10,000psi (mated), and composed of twelve individual contacts rated up to 600VDC. In the event of an internal pressure buildup beyond 5–15psi, a pressure relief valve would vent to prevent explosion. Four metal posts were attached to the exterior of this section, providing a docking mechanism for ensuring secure transport of the MSLED until manual deployment from the mothership.

An internal support structure serving as a modular and reconfigurable frame was located within this front compartment allowing internal components to be firmly mounted. This structure was composed of three subsections each 3D-printed from Accura 60 or SL 7820 plastic similar to ABS. The internal structure also included two aluminum support rings which prevented buckling of the exterior hull under pressure. The front subsection of the internal structure contained the camera and the inertial measurement unit; the middle subsection contained batteries and the speed controller; and the rear subsection contained the command and data handling board and fibre transceiver (Fig 3). The middle section accommodated the battery pack in order to adjust the overall centre of mass; this gave the operator control of the pitch. The system was controlled by a Hitec HS-35HD servo modified for continuous rotation.

The flooded fibre bay housed an optical fibre spool that automatically deployed fibre when under tension. Since this chamber was not pressurised it was printed from DuraForm PA plastic. A similar

fibre-optic deployment mechanism had been successfully utilised previously within an analogous underwater vehicle (Bowen et al., 2008).

The rear tail-cone was machined from Syntech AM-30B high-density buoyant foam and was composed of two subsections: a pressure-compensated servo section that housed the four servo motors used to actuate the steering fins and a flooded motor section that housed a sealed brushless motor used to drive the main propeller (Fig 3). The former was filled with low-viscosity silicone oil ($[-\text{Si}(\text{CH}_3)_2\text{O}-]^n$) as a pressure compensation liquid and this was sealed behind a flexible polyurethane membrane.

A mass budget for the vehicle is given in Table 2.

4.2. Instrumentation

The MSLED was equipped with a high-definition video camera as well as sensors for measuring salinity, temperature and depth. It also included additional interface ports that allowed for expansion of the sensing package. An Allied Vision Prosilica GC-1380C high definition video camera utilising a Sony ICX-285 2/3" CCD sensor was selected for the low-light environment because it had a large sensor area of $41.6025\mu\text{m}^2$. This camera was capable of capturing video at a maximum resolution of $1,360 \times 1,024$ pixels at a frame rate of 20 frames per second and broadcast the data stream via Gigabit Ethernet. Additionally, the camera provided an RS-232 interface for a bidirectional serial communications stream over the same Gigabit Ethernet connection and this was utilised as the command and data handling

Table 2: Itemised MSLED mass budget

Component	Quantity	Unit mass (g)
AVT Prosilica GC-1380C	1	104
Deepsea Power & Light 701-00006	1	11.7
Exceed RC Optima 300 2208-1100KV	1	50
Kowa LM6JC	1	63
Moog Prizm TEL Series Gigabit	1	62
Microstrain 3DM-GX3-25	1	18
Hitec HS-35	5	4.5
RECOM RCD-24-1.00/W/X3	2	6.8
Saft LSH-14	8	51
Sanmina Fibre Spool	1	155
Star-Oddi DST CTD	1	35
Swiss Jewel W51.00	1	52
Teledyne Impulse IE55-1206-CCP	5	4.4
CDH Board	1	71
Light Ring	1	12
Nosecone	1	174
Internal Structure	1	155
Support Rings	2	18.5
Pressure Hull	1	710
Fibre Section	1	178
Tail Section	1	208
Silicone Oil	1	26
Cabling, screws, etc.	1	300
Total		2,887

interface with the surface. The camera had a compact form factor of $33 \times 46 \times 59$ mm and a mass of 104g without a lens, and consumed up to 3.3W at 5V. A Kowa LM6JC lens was fitted to this camera along with an f-stop adjustment servo, allowing for variation of the iris range from $f/1.4$ to $f/16$.

Underwater illumination was provided by a custom-designed light ring of six 100lm Cree XLamp XP-E2 light emitting diodes (LEDs), with each emitting up to 283lm at 3.15W on an aluminum-backed printed circuit board. These LEDs were wired up in a parallel-series configuration of three LEDs per string and were driven by two RECOM RCD-24-1.00/W/X3 LED drivers at 1A supporting independent control of each LED string by the control board using pulse-width modulation (PWM). Each LED was fitted with a 30° Ledil Lisa2 miniature lens and potted within approximately 1cm of MG Chemical Optically Clear epoxy for waterproofing.

A custom Star-Oddi DST CTD miniature salinity, temperature and depth recorder was modified for online operation. With dimensions of only 15mm in diameter and 46mm in length, the CTD was installed externally within the rear tail section Kort-nozzle assembly and was rated for a depth of up to 2,000m. The CTD unit was calibrated for conductivity measurements from $3\text{--}37\text{mS cm}^{-1}$ at an accuracy of 4% full-scale resolution (type I), and also had the capability to be calibrated for $0.5\text{--}8\text{mS cm}^{-1}$ low conductivity environments at an accuracy of 6% of the full-scale resolution (type L).

4.3. Communication

A fibre-optic communication system was used based on the bandwidth and transmission requirements. The MSLED was connected to the mothership via 1.2km of $80\mu\text{m}$ single-mode optical fibre that was stored within a dedicated fibre bay onboard the vehicle. The fibre, custom-manufactured by Sanmina, was precision wound with an internal reverse twist which allowed kink-free deployment from the rear of the vehicle by the drag of the water. This maintained stress levels below the fibre's tensile strength of up to 4.5kg. The mothership was connected to the surface through a custom Falmat Xtreme-Green tether which contained two single-mode optical fibres, two multi-mode optical fibres and three Kevlar strength members.

In order to convert between Gigabit Ethernet and fibre-optic signals a pair of Moog Prizm TEL Series Gigabit media converters was used as fibre-optic transceivers, achieving an optical data rate of up to 1.25Gbps. These transceivers operate at 1,550nm and 1,310nm wavelengths, respectively, and were capable of transmitting optical signals up to 50km of single-mode fibre while consuming a maximum of 3W at 5V.

Internal communication within the MSLED occurred either over a Cat6 Gigabit Ethernet cable between the fibre transceiver and camera or an Electronics M22759/43-22-9 dual wall ETFE 22AWG copper wire for strictly internal connections. This is shown in Fig 4.

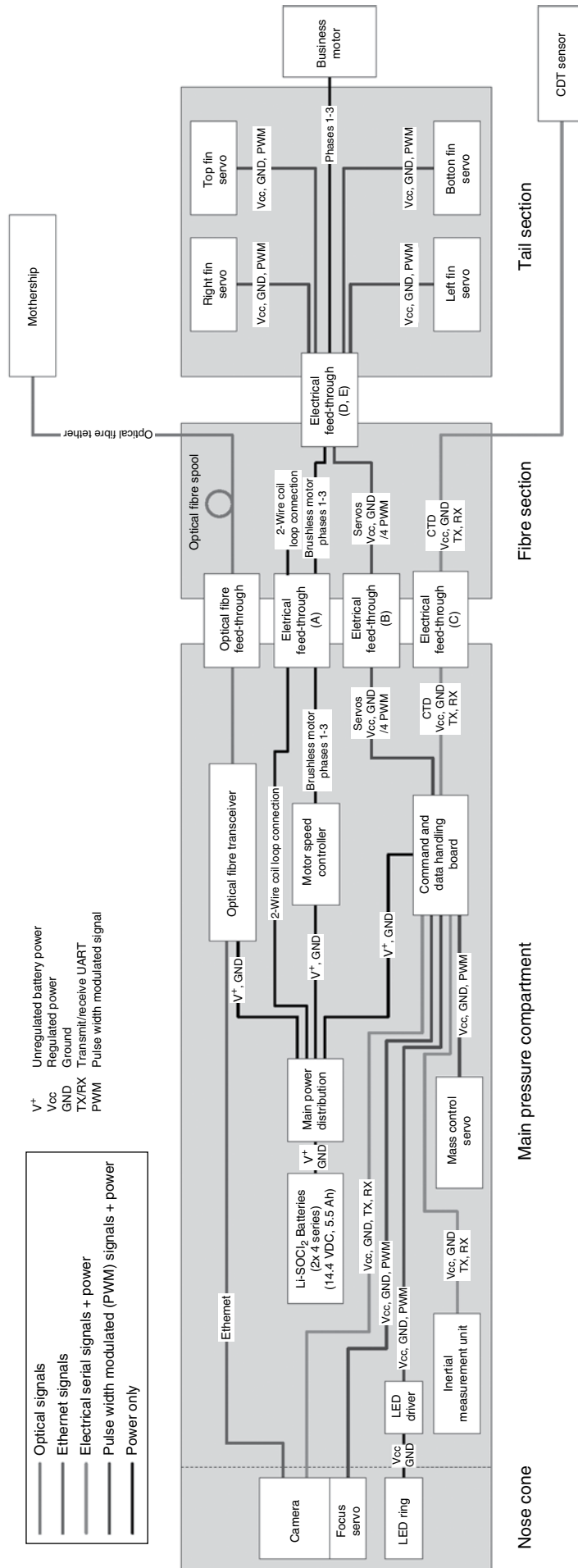


Fig 4: System diagram of the MSLED showing interconnections between the three distinct vehicle sections

4.4. Command and data handling

The command and data handling (CDH) subsystem interfaced between the ground station at the surface and all the electrical components on the MSLED. It was responsible for translating user-commands from the ground station into control signals that were sent to the motor, servos, lights, camera and assorted subsystems. In addition, the system collected and transmitted sensor and house-keeping data back up to the surface.

The CDH capabilities were provided by an Atmel ATmega2560 microcontroller that was capable of operating at up to 16 million instructions per second (MIPS) at less than 5mW. It was equipped with 256 kilobytes of flash memory for the CDH software, 8kb of runtime SRAM, 4kb EEPROM and supported a maximum of 86I/O pins as well as 4 serial USARTs. An internal 10-bit A/D converter was used to measure battery voltage and current consumption via a shunt resistor.

4.5. Power

Eight Saft LSH-14 LiSOCl₂ lithium primary batteries, each rated for 5.8Ah at 3.6V, supplied onboard power; these were connected such that four cells in series formed a pack, and two packs were connected in parallel. This resulted in a nominal output of 14.4V with a capacity of 11Ah for approximately 158.4Wh of total battery energy. An itemised power budget is listed in Table 3 showing a total maximum power consumption of 94.4W. 24AWG enamel-coated copper wire penetrated the external bulkhead and provided power connections to the lights.

The MSLED was powered by three internal rails rated for 6A at 5V, 3A at 5V, and 3A at 10V, which were used respectively for powering the servos, general electronics and lighting subsystem. Texas Instruments PTN78020W and PTN78060W switching buck regulators, which achieve up to 96% efficiency, performed power regulation and voltage step-down. In addition, the 10V rail was backed by three Tecate PC5-5 2F supercapacitors to ensure stable voltage regulation even under transient

Table 3: Itemised MSLED power budget

Component	P _{max} (W)
AVT Prosilica GC-1380C	3.3
CDH Board	0.75
Cree XLamp XP-E2	18.9
Exceed RC Optima 300 2208-1100KV	65
Moog Prizm TEL Series Gigabit	3.0
Microstrain 3DM-GX3-25	0.4
Hitec HS-35	3.0
Star-Oddi DST CTD	0.05
Total	94.4

conditions. In order to further conserve power, each electrical subsystem was connected to a Vishay Si4838DY MOSFET, which could be switched on/off by the CDH board. Finally, an external loop-back connector enabled the MSLED to be turned on and off without opening the vehicle; this is shown in Fig 4.

4.6. Navigation

Coarse navigation and georeferencing of scientific measurements was determined via a MicroStrain 3DM-GX3-25 inertial measurement unit (IMU), which incorporated an internal triaxial accelerometer, a triaxial gyroscope and a triaxial magnetometer. Since the accumulated integration error of acceleration for position did not allow precise positioning, only estimates of the vehicle's attitude and heading were displayed as a navigational aid for the operator.

4.7. Propulsion and steering

Owing to the size constraints of the vehicle, a single Exceed RC Optima 300 2208-1100KV brushless motor attached to a propeller provided propulsion. Motor speed was controlled by a Castle Creations Mamba Max Pro electronic speed controller which supported a user-programmable brake curve and low-voltage cutoff. Steering was achieved through four steering fins controlled independently by Hitec HS-35HD servos.

The external propeller and fin assembly provided a mounting point for the miniaturised CTD sensor, a guard rail around each steering fin to prevent potential damage from object impact and incorporated a Kort-type nozzle around the propeller to optimise water flow. In addition, the presence of a guide rail located at the cable attachment point also protected against the fibre-optic cable becoming ensnared around the fins and propeller. This design allowed the MSLED to effectively control its pitch, yaw and roll, while automatically centring the roll angle to neutral caused by the inherent low centre of vehicle mass.

4.8. Surface control

Ground control software for the MSLED was written in C# and utilised the XNA framework to communicate with an XBOX360 controller that was used to pilot the vehicle. Video footage from within the subglacial lake was shown on the display overlaid with information about the vehicle's thrust, heading and pitch, as well as internal temperature, humidity, voltage and current. Additional features included the ability to put the vehicle into a low-power mode by selectively powering down certain peripherals, as well as recording all serial and video

communications from the vehicle. This software is open source and publicly available at www.github.com/msled/EERILControlSystem.

4.9. Mothership

From a high-level perspective, the mothership shared a similar architecture to that of the MSLED (Fig 2). A Prevco A621 aluminum hull, rated to 2,100m, provided a pressure-sealed electronics compartment that also included a front window for the camera. A GoPro HERO3+ Black Edition served as the primary downward-facing video camera, while an external side-facing SplashCam Delta Vision provided a second perspective. An Arduino Mega 2560 with an attached Ethernet Shield was used to interface with the surface control software that allowed for remote control of the lights and monitoring of the onboard Crossbow CXTD02 inclinometer and Seabird SBE50 depth sensor.

Four Reedy WolfPack lithium polymer batteries provided power. An Astro Battery Balancer connected to each battery facilitated external charging through a Teledyne Impulse IE55-1206-CCP penetrator without having to disassemble the mothership. Two LM2596 DC-DC voltage converters regulated internal rails rated for 5V at 3A and 12V at 3A, and a Croydom DMO063 solid state relay was used to control the lights, which were regulated by LUXdrive BuckBlock A009-D-V-2100 drivers.

Twelve Cree XLamp XM-L2 LEDs provided lighting, four front-facing and eight side-facing, potted within MG Chemical Optically Clear epoxy. Each LED supported a maximum luminous output of over 1000lm at 10W and emitted a cool white light that propagated well under water. To assist with the return of MSLED to the mothership, the lights were strobed to serve as an optical beacon and illuminated the environment for the front and side-facing cameras (Fig 3).

Two Fibrelink 3105 Beamer-V fibre converters were coupled to separate multi-mode fibres in order to transmit video footage from the cameras to the surface. Additionally, a Black Box LHC029A-R2 miniature media converter was used to transmit the Ethernet connection from the Arduino onto a single-mode fibre.

A docking mechanism utilising four latches was used to attach the MSLED vertically below the mothership. This mechanism completely restrained the MSLED, preventing it from detaching until all four fins of the MSLED individually trigger each release.

5. Testing

A number of tests were performed in order to verify and validate the implementation of the design.

5.1. Structural

Maintaining structural integrity at depth was essential for the survival of MSLED. Initial pressure tests of the prototype design revealed that a 3mm sapphire window was insufficient. Later pressure tests also revealed that the structural integrity of the aluminum support rings was compromised by the threaded holes used to fasten subsections of the interior structure together; this resulted in an implosion of the main hull under pressure. After increasing the thickness of the sapphire window to 6mm, and removing the threaded holes from the support rings, subsequent pressure testing was successfully performed to 117.2bar or an equivalent depth of approximately 1.2km. Nevertheless, metal fatigue caused by cyclical stressing has still to be mitigated; failure testing showed that approximately 10 cycles of pressure testing at 117.2bar still caused hull implosions even with the new design.

5.2. Instrumentation, communication and CDH

The media conversion chain that provided two-way communication between the MSLED and the ground station was composed of the following phases: (1) serial data from and to the command and data handling subsystem, along with high-definition video from the camera; (2) electrical transmission through a copper Gigabit Ethernet cable; (3) electro-optic conversion by a fibre-optic transceiver; (4) optical transmission through the MSLED onboard optical fibre; (5) coupling of the optical fibre at the mothership; (6) optical fibre as part of a tether connection with the surface; (7) optoelectric conversion by a fibre-optic transceiver to Gigabit Ethernet signals; (8) packet decoding by control software on the ground station; as well as (9) the displaying of live video.

This chain was verified both in the laboratory as well as during Antarctic testing in 2012–2013. It consisted of a 1.2km single-mode fibre connecting the MSLED and its mothership coupled to a 1.3km single-mode fibre within a custom-manufactured tether connecting the mothership and the surface control station. This produced a total fibre length of approximately 2.5km. A video stream with a $1,360 \times 1,024$ pixel resolution was transmitted successfully at a rate of 20 frames per second in parallel with serial data of up to 115kbps over the entire communication chain.

5.3. Temperature and battery performance

The physical extremes of the Antarctic environment generated significant functional challenges on the vehicle's components. A low temperature test was conducted to verify the functionality of crucial components and to characterise battery performance

in these conditions. The test was performed both in the laboratory and during the 2012–2013 Antarctic season with the optical fibre as the only external connection. Environmental temperature ranged from 0°C to –4°C resulting in an ice-water slush mix. Under these conditions the batteries powered the vehicle continuously for approximately 170 minutes at idle.

Power testing for the mothership was also performed in the laboratory at room temperature with all the mothership lights turned on. Under those conditions, the system ran for approximately four hours without reaching the minimum discharge voltage; that performance was considered sufficient for deployment even with a 50% deterioration in power caused by the low temperatures.

5.4. Mothership

Since communications with MSLED interfaced through the mothership this system underwent significant testing. In the process it was discovered that improper handling of the mothership could result in damage to the external penetrator for the fibre-optic tether, requiring the entire component to be replaced. As a result, the internal systems were redesigned to support external charging and data access eliminating the requirement for frequent disassembly of the mothership hull between deployments.

Extensive testing of the new mechanism in various pools and at the University of Maryland's Space Systems Laboratory improved the reliability of the docking mechanism.

5.5. End-to-end

End-to-end testing prior to Antarctic deployments occurred at Lake Tahoe, Bartlett Lake, University of Maryland's Space Systems Laboratory, Monterey Bay Aquarium Research Institute, and various other locations.

During end-to-end testing in Lake Tahoe, it was discovered that MSLED experienced internal condensation, leading to fogging of the front window that obscured the internal camera. High-performance t.h.e. desiccant supplied by EMD Millipore was suspended within braided sleeving pouches attached to the internal structure; this achieved up to 35% water adsorption by weight. The presence of indicating agents signalled when water adsorption exceeded 13%, at which point the desiccant was regenerated by prolonged heating and reused. This approach resolved the condensation problem permanently without requiring additional heating or purging.

The first end-to-end testing of MSLED with the mothership occurred at the Space Systems Laboratory

of the University of Maryland. Within their Neutral Buoyancy Research Facility, the MSLED and mothership were tested as a system to a depth of 7.3m for correct operation. Darkening of the entire facility verified that the mothership lights were sufficient to illuminate the environment for MSLED navigation to a distance of 15.2m.

6. Antarctic deployments

Initial deployments to Antarctica occurred as part of the WISSARD expedition during the 2011–2012 and 2012–2013 Antarctic summer seasons.

6.1. McMurdo Sound

A full end-to-end trial deployment of the prototype MSLED vehicle and mothership occurred under the sea ice near McMurdo Station in Antarctica (Fig 5). With the exception of environmental pressure, this locale provided an analogous environment to a subglacial lake, with approximately 3m of sea ice preventing light infiltration into subsurface water and maintaining a water temperature of around –1.9°C. Finally, the sea ice environment necessitated the use of deployment procedures similar to the ones to be applied for accessing SLW.

Deployment under the sea ice occurred a total of five times, with each test mission lasting on average 45 minutes. During this time, one prototype vehicle was lost in a borehole caused by problems with the deployment mechanism; this resulted in a more secure redesign. Nevertheless, the prototype vehicle demonstrated that it could be controlled through a fibre-optic communication link to the surface while simultaneously proving its maneuverability by diving down to the sea floor to capture video of the aquatic life. In addition, it was shown that a two-man team could deploy the MSLED, with all the equipment carried manually to the deployment site.



Fig 5: External view of the MSLED taken by a diver in McMurdo Sound

6.2. Subglacial Lake Whillans

During the 2012–2013 Antarctic summer season, MSLED and its mothership were deployed at the Whillans Ice Stream as part of the WISSARD expedition. After drilling a borehole of approximately 0.6m diameter, the mothership was deployed five times for visual inspection. Although the air/water interface occurred at 78m below the ice surface, initial inspection revealed the presence of two divergent boreholes owing to improper hot-water drill alignment (Fig 6). After correcting this error and re-drilling, video inspection showed a significant increase in water turbidity beginning at about 520m depth, before penetrating SLW at $800 \pm 1\text{m}$ below the surface (Christner et al., 2014), equivalent to earlier estimates provided by ground-penetrating radar and seismic surveying.

As the first ever man-made vehicle to enter SLW, the mothership captured unique lakefloor footage of the environment. Video evidence determined that previous lake depth predictions were incorrect, as SLW was found to be a relatively shallow lake of about 2.2m depth with significant soft sediment that obscured visibility (Fig 7; Tulaczyk et al., 2014). However, whereas the potential risk of borehole diameter shrinkage caused by refreezing was planned for, the formation of ice at the air-water interface in the borehole was not. This resulted in

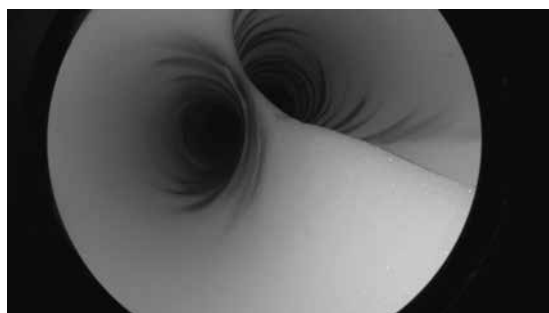


Fig 6: Video from the mothership showing multiple divergent boreholes



Fig 7: Video from the mothership showing the floor of SLW

significant disturbance to the planned operational sequence because by the time that MSLED entered the borehole the ice layer, estimated to be at least 3cm thick, prevented further entry into SLW. In a last-ditch attempt to reopen the borehole, drill water was injected from the surface to melt this ice layer (Tulaczyk et al., 2014). However, this rapid change in water temperature resulted in a stress fracture of multiple fibre-optic cables within the tether, causing a loss of communications and terminating the deployment.

6.3. Lessons learned

During deployment, the WISSARD expedition experienced a number of challenges associated with borehole drilling that strongly resemble those encountered previously by the British at Subglacial Lake Ellsworth (ESL). In particular, both expeditions had problems with borehole divergence that was most likely caused by non-vertical borehole drilling orientation. Although the presence of two divergent boreholes only resulted in a temporary setback for the WISSARD expedition (Fig 6), the failure of the main borehole to link with a subsurface cavity of water at ESL ultimately resulted in the premature termination of the expedition. However, there were other compounding factors such as lack of sufficient fuel and electrical failures in the boiler control board (Siegert et al., 2014). As recommended by the Failure Review Board for the Lake Ellsworth Programme the authors of the present paper agree that the presence of a down-borehole camera is very useful for examining borehole integrity and should, preferably, be incorporated into the design of the drilling equipment. This would be an improvement from using a separate instrument, such as the mothership, because of the delays associated with equipment decontamination and deployment/retrieval of such into the borehole.

Likewise, the problems encountered by the MSLED team and the WISSARD expedition with prolonged through-borehole deployment indicate that greater consideration is required to prevent borehole closure. In particular, while both expeditions were prepared for lateral borehole closure through ice creep (Siegert et al., 2014; Tulaczyk et al., 2014), it appears that neither was prepared for the borehole refreezing at the air-water interface. Calculations by Tulaczyk et al. (2014) estimate that borehole ice growth is approximately 3cm day^{-1} which is of sufficient thickness to support equipment with a mass of up to 200kg. As a result, continuous injection of 1L min^{-1} of drill water at 85°C into a 0.6m diameter borehole is necessary to prevent surface ice from exceeding a thickness of 0.2cm which can be broken easily by equipment

with mass exceeding 2kg. Not only does this require an additional hose in the borehole, which can risk entanglement, but it may also require instrumentation to survive a sudden change in water temperature of approximately 85–95°C as demonstrated by the failure of the MSLED tether.

Based on readings from a SeaBird CTD sensor deployed by the WISSARD expedition, it is likely that the low conductivity of the subglacial lake at $720 \pm 10 \mu\text{S cm}^{-1}$ would have caused the MSLED Star Oddi CTD to emit erroneous readings because of its calibration range of 3–37mS cm^{-1} , had MSLED been able to enter SLW (Christner et al., 2014). For future subglacial deployments, the Star Oddi CTD should at least be calibrated for a lower conductivity range of 0.5–5mS cm^{-1} . However, given the 6% full-scale conductivity accuracy at that range, it may be necessary to consider a custom calibration range or alternative CTD. Likewise, given that the salinity measurements from the CTD were computed from the conductivity reading based on The Practical Salinity Scale 1978 (PSS-78), it is important to understand that these measurements were relative to a standard KCl solution, and may need to be reevaluated given the nonstandard subglacial lake ionic concentrations (Christner et al., 2014).

The loss of a prototype MSLED vehicle in McMurdo Sound resulted in suggestions that a mothership docking system based on a hook and line system could result in unintended disconnection caused either by impact or vibration. As a result, the docking system was redesigned to clamp onto four metal posts attached to the exterior of the MSLED tail section, preventing deployment until all posts were released simultaneously through the movement of all tail servos.

7. Conclusions

The MSLED is a unique submersible owing to the combination of (a) a small form factor of 14cm in diameter that makes it suitable for deployment through slim boreholes; (b) the scientific core functionality to record high-resolution video as well as conductivity, temperature and depth (with options for additional environmental data sensors); (c) a ruggedised system that is pressure-rated to operate at a depth of 1,200m, with an operational distance of up to 1,000m from the borehole entrance, and temperature-rated to operate for a minimum of two hours at Antarctic water temperatures; and (d) the extensive use of commercial off-the-shelf components, significantly reducing development costs and production time.

The MSLED was tested extensively in a variety of environments, including test laboratories, freshwater

surface lakes and saltwater polar ice shelves. Test results confirmed the compliance with operational requirements as well as design constraints, and further showed that the MSLED is capable of exceeding its specifications, allowing for flexibility in deployment to other similar aquatic analogues with different applications. After the MSLED's initial deployment in McMurdo Sound and trial at SLW, the design is currently being optimised for subsequent field seasons in Antarctica.

Acknowledgements

This research is dedicated to the memory of Dr Alberto Behar, who passed away tragically on January 9, 2015.

The work described in the present paper was initially carried out at the Jet Propulsion Laboratory, managed by the California Institute of Technology under contract to the National Aeronautics and Space Administration, and subsequently at the School of Earth and Space Exploration at Arizona State University. Grant funding was provided by the NASA Earth Science Cryospheric Sciences Program and the National Science Foundation under award #1142123, with internships and research visits supported by the Jet Propulsion Laboratory, Arizona Space Grant Consortium, German Academic Exchange Service and Technische Universität München.

Testing of vehicle subsystems occurred at the Jet Propulsion Laboratory, Arizona State University, Deepsea Power & Light and Prevco. Full end-to-end testing was performed at various facilities, including the University of Maryland's Space Systems Laboratory, McMurdo Station at the Antarctic Ross Ice Shelf, the Monterey Bay Aquarium Research Institute, Bartlett, Lake Tahoe, and the Sun Devil Fitness Complex and various other pools around Arizona State University.

Machining of the vehicle was performed by the Instrument and Prototype Machine Shop at Arizona State University, with anodising of the hull and pressure bulkheads performed by Southwest Metal Finishing and Anodizing of Mesa. 3D printing of internal components was handled by the Digital Lab at the Herberger Institute at Arizona State University, Phoenix Analysis and Design Technologies (PADT) and Shapeways.

The authors would also like to thank past contributors who worked on this project, namely Anna Camery, Cedric Cocard, Amanda Duffy, Andrew Elliott, Chris Gay, Jonathon Houda, Toby Jacobson, Alex Kafka, Puja Kapoor, Javed Khan, Michael King, Stephanie Lauk, Prasad Naik, Tom Nordheim, Evan Olson, Karthik Pappu, Andres Mora Vargas and Eric

Weger. In addition, the authors are grateful to Matthias Butenuth, Lisa Clough, Berglind Helgadóttir, Tom Wagner, Mary Voytek, Luther Beegle, Pamela Brown, Jonathan Houda, Shashank Bhavanashi, Teresa Robinette, Connie Seidel, Florian Seitz, Jessie Crain, Sonia Esperanca, Fredrik Bruhn, Haraldur Hilmarsson, Cal Peters, Ken Mankoff, Alexandra Isern, Lillie Glenn and Dana Yoerger for their support. Finally, the authors would like to thank all members of the WISSARD expedition for making deployment to the Whillans Ice Stream in Antarctica a reality.

The authors are also grateful for the comments and suggestions provided by the reviewers, whose feedback has helped improve this manuscript.

References

- Alley RB. (2001). *The West Antarctic Ice Sheet: Behavior and Environment*. Washington, DC: American Geophysics Union, 296pp.
- Antonelli G, Fossen TI and Yoerger DR. (2008). Underwater Robotics. In: Siciliano B and Khatib O. (eds.). *Springer Handbook of Robotics*. Germany: Springer, 987–1,008.
- Bamber JL, Riva REM, Vermeersen, BLA and LeBrocq AM. (2009). Reassessment of the potential sea-level rise from a collapse of the west Antarctic ice sheet. *Science* **324**: 901–903.
- Behar AE, Walter C, Nordheim T, Ho C, Camery A, Elliott A, Olson E, Kapoor P, Khan J and Naik P. (2010). Development of a micro subglacial lake exploration device. *American Geophysical Union Fall Meeting Abstracts* A522.
- Blythe DS, Duling DV and Gibson DE. (2014). Developing a hot-water drill system for the WISSARD project: 2. In situ water production. *Annals of Glaciology* **55**: 298–302.
- Bowen AD, Yoerger DR, Taylor C, McCabe R, Howland J, Gomez-Ibanez D, Kinsey JC, Heintz M, McDonald G, Peters DB, Fletcher B, Young C, Buescher J, Whitcomb LL, Martin SC, Webster SE and Jakuba MV. (2008). The Nereus hybrid underwater robotic vehicle for global ocean science operations to 11,000m Depth. Proceedings of the 2008 IEEE/MTS Oceans Conference, September 2008. Quebec City, Quebec. DOI: 10.1109/OCEANS.2008.5151993.
- Burnett J, Rack FR, Blythe DS, Swanson P, Duling DV, Gibson DE, Carpenter C, Roberts G, Lemery J, Fischbein S and Melby A. (2014). Developing a hot-water drill system for the WISSARD project: 3. Instrumentation and control systems. *Annals of Glaciology* **55**: 303–310.
- Cazenave F, Zook R, Carroll D, Flagg M and Kim S. (2011). Development of the ROV SCINI and deployment in McMurdo Sound, Antarctica. *Journal of Ocean Technology* **6**: 39–58.
- Christianson K, Jacobel RW, Horgan HJ, Anandakrishnan S and Alley RB. (2012). Subglacial Lake Whillans – Ice-penetrating radar and GPS observations of a shallow active reservoir beneath a West Antarctic ice stream. *Earth and Planetary Science Letters* **331**: 237–245.
- Christner BC, Royston-Bishop G, Foreman CM, Arnold BR, Tranter M, Welch KA, Lyons WB, Tsapin AI and Priscu JC. (2006). Limnological conditions in Subglacial Lake Vostok, Antarctica. In: *Limnology and Oceanography* **51**: 2,485–2,501.
- Christner BC, Priscu JC, Achberger AM, Barbante C, Carter SP, Christianson K, Michaud AB, Mikucki JA, Mitchell AC, Skidmore ML and Vick-Majors TJ. (2014). A microbial ecosystem beneath the West Antarctic Ice Sheet. *Nature* **512**: 310–313.
- Domack E, Ishman S, Leventer A, Sylva S, Willmott V and Huber B. (2005). A chemotrophic ecosystem found beneath Antarctic ice shelf. *Eos Transactions American Geophysical Union* **86**: 269–272.
- Fricker HA, Scambos T, Bindschadler R and Padman L. (2007). An active subglacial water system in west Antarctica mapped from space. *Science* **315**: 1,544–1,548.
- Fricker HA, Powell R, Priscu JC, Tulaczyk S, Anandakrishnan S, Christner BC, Fisher AT, Holland D, Horgan H, Jacobel R, Mikucki J, Mitchell A, Scherer R and Severinghaus J. (2011). Siple Coast Subglacial Aquatic Environments: The Whillans Ice Stream Subglacial Access Research Drilling Project. In: *Antarctic Subglacial Aquatic Environments*. Washington, DC: Wiley, 199–219.
- Gray L, Joughin I, Tulaczyk S, Spikes VB, Bindschadler R and Jezek K. (2005). Evidence for subglacial water transport in the west Antarctic ice sheet through three-dimensional satellite radar interferometry. *Geophysical Research Letters* **32**: L03501.
- Horgan HJ, Alley RB, Christianson K, Jacobel RW, Anandakrishnan S, Muto A, Beem LH and Siegfried MR. (2013). Estuaries beneath ice sheets. *Geology* **41**: 1,159–1,162.
- Kamb B. (1987). Glacier surge mechanism based on linked cavity configuration of the basal water conduit system. *Journal of Geophysical Research: Solid Earth* **92(B9)**: 9,083–9,100.
- Karl DM, Bird DF, Bjorkman K, Houlihan T, Shackelford R and Tupas L. (1999). Microorganisms in the accreted ice of Lake Vostok, Antarctica. *Science* **286**: 2,144–2,147.
- Lanoil B, Skidmore M, Priscu JC, Han S, Foo W, Vogel SW, Tulaczyk S and Engelhardt H. (2009). Bacteria beneath the west Antarctic ice sheet. *Environmental Microbiology* **11**: 609–615.
- Lorenz RD, Gleeson D, Prieto-Ballesteros O, Gomez F, Hand K and Bulat S. (2011). Analog environments for a Europa lander mission. *Advances in Space Research* **48**: 689–696.
- Mowlem MC, Tsaloglou MN, Waugh EM, Floquet CF, Saw K, Fowler L, Brown R, Pearce D, Wyatt JB, Beaton AD, Brito MP, Hodgson DA, Griffiths G, Bentley M, Blake D, Capper L, Clarke R, Cockell C, Corr H, Harris W, Hill C, Hindmarsh R, King E, Lamb H, Maher B, Makinson K, Parnell J, Priscu JC, Rivera A, Ross N, Siegert MJ, Smith A, Tait A, Tranter M, Wadham J, Whalley B and Woodward J. (2011). Probe technology for the direct measurement and sampling of Ellsworth Subglacial Lake. *Antarctic Subglacial Aquatic Environments*, 159–186.
- Priscu JC and Christner BC. (2004). Earth's icy biosphere. In: Bull A. (ed.). *Microbial Diversity and Bioprospecting*. Washington, DC: American Society for Microbiology Press, 130–145.
- Priscu JC, Achberger AM, Cahoon JE, Christner BC, Edwards RL, Jones WL, Michaud AB, Siegfried MR, Skidmore ML, Spiegel RH, Switzer GW, Tulaczyk S and Vick-Majors TJ. (2013). A microbiologically clean strategy for access to the Whillans ice stream subglacial environment. *Antarctic Science* **25**: 637–647.
- Rack FR, Duling DV, Blythe DS, Burnett J, Gibson DE, Roberts G, Carpenter C, Lemery J and Fischbein S. (2014). Developing a hot-water drill system for the

- WISSARD project: I. Basic drill system components and design. *Annals of Glaciology* **55**: 285–297.
- Richmond K, Febretti A, Gulati S, Flesher C, Hogan BP, Murarka A, Kuhlman G, Sridharan M, Johnson A, Stone WC, Priscu JC and Doran P. (2011). Sub-ice exploration of an Antarctic lake: results from the Endurance Project. 17th International Symposium on Unmanned Untethered Submersible Technology. Portsmouth, NH. Available at www.evl.uic.edu/documents/subiceexploration_uast11.pdf; last accessed <29 May 2015>
- Siegert MJ, Carter S, Tabacco I, Popov S and Blankenship D. (2005). A revised inventory of Antarctic subglacial lakes. *Antarctic Science* **17**: 453–460.
- Siegert MJ, Makinson K, Blake D, Mowlem M and Ross N. (2014). An assessment of deep hot-water drilling as a means to undertake direct measurement and sampling of Antarctic subglacial lakes: experience and lessons learned from the Lake Ellsworth field season 2012/13. *Annals of Glaciology* **55**: 59–73.
- Smith BE, Fricker HA, Joughin IR and Tulaczyk S. (2009). An inventory of active subglacial lakes in Antarctica detected by ICESat (2003–2008). *Journal of Glaciology* **55(192)**: 573–595.
- Tulaczyk S, Mikucki JA, Siegfried MR, Priscu JC, Barcheck CG, Beem LH, Behar AE, Burnett J, Christner BC, Fisher AT, Fricker HA, Mankoff WISSARD at Subglacial KD, Powell RD, Rack F, Sampson D, Scherer RP and Schwartz SY. (2014). Lake Whillans, west Antarctica: scientific operations and initial observations. *Annals of Glaciology* **55**: 51–58.
- Vaughan DG and Arthern R. (2007). Why is it hard to predict the future of ice sheets? *Science* **315**: 1,503–1,504.
- Wingham DJ, Siegert MJ, Shepherd A, and Muir AS. (2006). Rapid discharge connects Antarctic subglacial lakes. *Nature* **440**: 1,033–1,036.
- Wright A and Siegert M. (2012). A fourth inventory of Antarctic subglacial lakes. *Antarctic Science* **24**: 659–664.
-